NJC

New Journal of Chemistry

An international journal of the chemical sciences

www.rsc.org/njc

Volume 33 | Number 8 | August 2009 | Pages 1621–1792

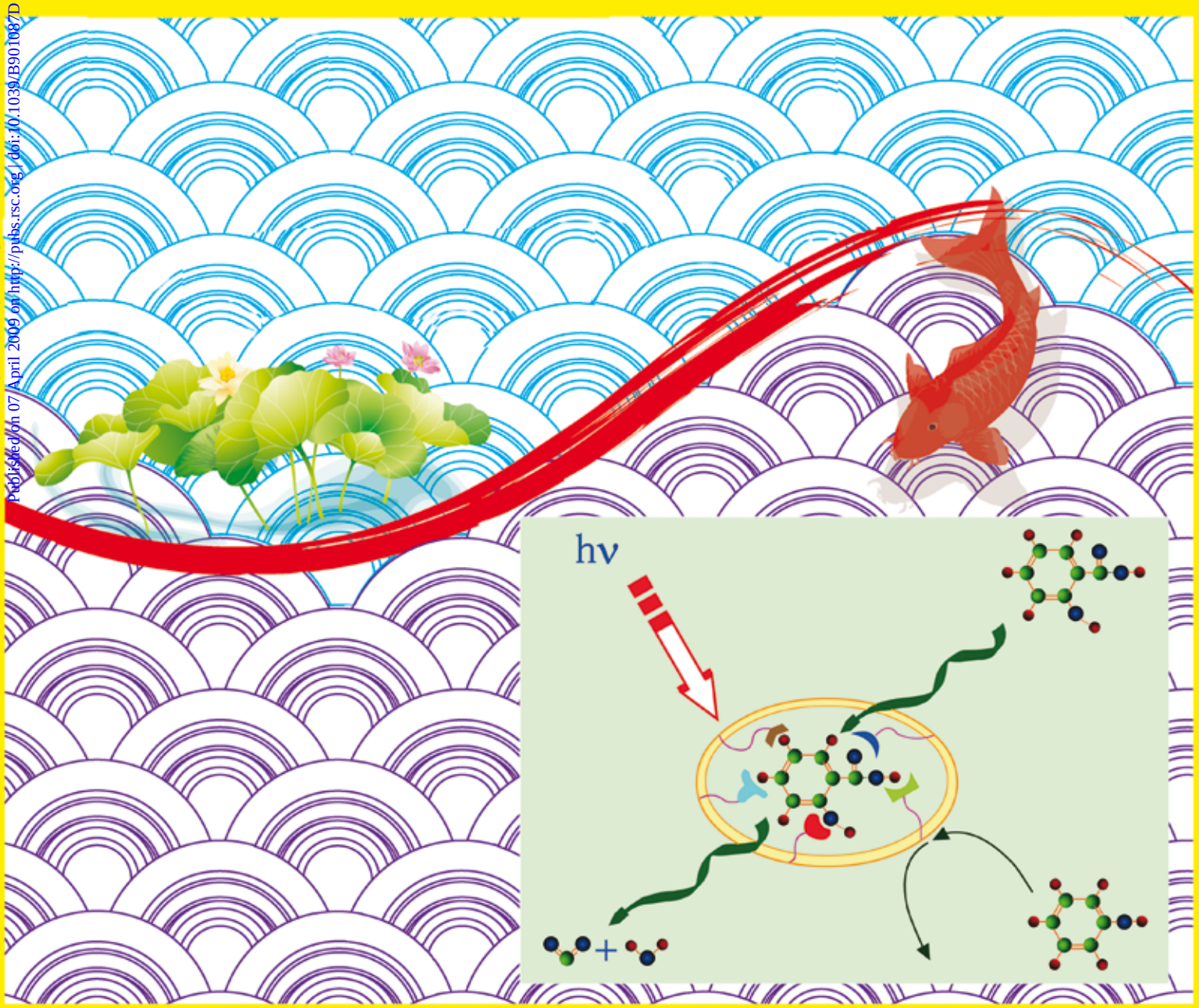

ISSN 1144-0546

RSC Publishing

cnrs

PAPER

Lihua Zhu, Heqing Tang *et al.*

Selective photocatalysis on molecular imprinted TiO_2 thin films prepared *via* an improved liquid phase deposition method

Selective photocatalysis on molecular imprinted TiO_2 thin films prepared *via* an improved liquid phase deposition method

Xiantao Shen,[a] Lihua Zhu,*[a] Hongwei Yu,[a] Heqing Tang,*[a] Shushen Liu[b] and Weiying Li[b]

Received (in Victoria, Australia) 19th January 2009, Accepted 25th February 2009
First published as an Advance Article on the web 7th April 2009
DOI: 10.1039/b901087d

Molecular imprinted thin films (MIFs) of TiO_2 were prepared with a liquid phase deposition (LPD) method, and characterized by FT-IR spectroscopy, UV-visible solid-state reflection spectroscopy, X-ray diffraction, and scanning electron microscopy. Among different approaches of removing the template in the preparation of MIFs, a calcination treatment was the best to produce more 3D "molecular footprint" cavities of the template on the MIF, which promoted further the photocatalytic activity of the MIF in comparison with the films pre-treated by extraction or photodegradation. Compared with the non-imprinted TiO_2 film (NIF), the MIF enhanced the photodegradation of the target pollutants by increasing the adsorption of the target pollutants on the surface of the MIF. From the Langmuir–Hinshelwood model, the value of the apparent reaction rate constant on the MIF was obtained, which was much larger than that on the NIF. The equilibrium adsorption constant on the MIF was more than 7 times that on the NIF. Because of this high affinity, the MIF exhibited special molecular recognition ability, leading to selective adsorption and photodegradation of the target pollutant. Moreover, the MIF was confirmed to have good stability during long-time photocatalysis.

1. Introduction

In recent years, the application of semiconductor-based photocatalysts has increasingly been used over the world to destroy environmentally toxic pollutants. Most of the research has focused on TiO_2, due to its low cost and excellent chemical stability against photocorrosion.[1,2] The use of nanoparticle suspension photocatalysts having high surface areas is advantageous for the adsorption of pollutants on the catalysts and for the utilization of the photons from the light source.[3] Nevertheless, nanopowder photocatalysts possess some defects such as being difficult to spread, easy to aggregate and they lose photocatalytic activity, and are difficult to reuse.[4,5] These defects may be further grandiose because nanoparticles were reported to show potential risks to humans.[6] Therefore, great efforts have been undertaken to immobilize TiO_2 on a substrate to form a thin film, which may show a promising application in the remediation of environmental pollution.[7]

The selectivity of photocatalysts is another important aspect in the photocatalytic technique, especially for the photodecomposition of target pollutants in the presence of other high-level pollutants.[8] Unfortunately, the photocatalytic oxidation of contaminants over TiO_2 is not selective because it is governed by a free-radical mechanism.[9] When TiO_2 is used to treat waste-water containing multiple pollutants, the low and/or non-toxic organic pollutants at high concentrations are firstly degraded, while the highly toxic organic pollutants at low concentrations are hardly removed by using the simple catalysts.[10] Therefore, the preparation of selective TiO_2 photocatalysts is interesting and essential to achieve selective removal of the highly toxic target pollutants. Ghosh-Mukerji *et al.* reported a TiO_2 photocatalyst combining photocatalytic and non-catalytic absorption domains. β-Cyclodextrin was used as the host on this composite photocatalyst, which effectively enhanced the photocatalytic degradation of organic pollutants such as benzene and 2-methyl-1,4-naphthoquinone in water.[11,12] We recently reported a nano-TiO_2 photocatalyst being surface modified by coating with molecule imprinted polymers (MIP), which were able to enhance photocatalytic degradation of the target molecules because it increased the selective adsorption of the specific pollutants.[13,14]

The MIP-coated TiO_2 nanoparticles are involved in some defects as conventional TiO_2 powders catalysts. These defects may be eliminated by preparing a molecular imprinted film (MIF). Because the available molecular imprinting technique cannot be simply used to prepare MIFs of TiO_2, we combine the liquid phase deposition method[15] and the surface molecular imprinting technique to prepare it in the present work. To prepare MIFs at a low temperature, P25 TiO_2 was added to the deposition solution as a crystallization revulsant.[16] During the preparation, the target pollutant was added as a template to the deposition solution, which will lead to the formation of footprint cavities on the film. Salicylic acid (SA) is chosen as a probe molecule to test the selectivity of the photocatalytic film, since it is an aromatic compound with a similar structure to the potential environmental pollutants.[17]

[a] *College of Chemistry and Chemical Engineering, Huazhong University of Science and Technology, Wuhan 430074, P.R. China. E-mail: lhzhu63@yahoo.com.cn, hqtang62@yahoo.com.cn; Fax: +86 27-87543632; Tel: +86 27-87543432*
[b] *Key Laboratory of Yangtze River Water Environment, Ministry of Education, College of Environmental Science and Engineering, Tongji University, Shanghai 200092, P.R. China*

2. Experimental

2.1 Materials

$(NH_4)_2TiF_6$, SA and phenol were supplied by Shanghai Chemical Reagent Company. Boric acid, NaOH, HNO_3 and HCl were provided by Tianjin Chemical Reagent Co., Ltd. All the chemicals were of analytical reagent grade and used as received without further purification. HPLC-grade methanol was obtained from Tedia and water was prepared by a Milli-Q-Plus ultra-pure water system. P25 TiO_2 nanoparticles (*ca.* 80% anatase, 20% rutile; BET area, *ca.* 50 $m^2\ g^{-1}$) were provided by Degussa (Germany).

2.2 Preparation of MIF

Commercial borosilicate glass (26 × 76 mm) was used as the substrate for preparing TiO_2 films. The glass was firstly immersed in an aqueous NaOH solution (2 mol L^{-1}) for 1 h to completely remove the organic contaminants on its surface. It was then cleaned ultrasonically by using water, HNO_3 (1 mol L^{-1}, 15 min), water (15 min), ethanol (15 min) and water (15 min) in turn, followed by thoroughly drying in air at 60 °C.

The conventional LPD method was improved to prepare the MIFs. Compared to the traditional approach,[18] two points were developed here. Firstly, a crystallization revulsant was added during the preparation to obtain a better crystal form for the photocatalysis. Secondly, three approaches for the removal of the template were proposed to eliminate the template completely and enhance the selectivity of the MIF. Accordingly, a solution (200 mL) containing 0.05 mol L^{-1} $(NH_4)_2TiF_6$ and 0.15 mol L^{-1} boric acid was prepared, and the pH was adjusted to pH 2.7 by adding HCl (2 mol L^{-1}). Into the solution, SA (as the template, 20 mmol L^{-1}) and P25 (as crystallization revulsant, 0.04 g L^{-1}) were added, followed by stirring to maintain the suspension. The freshly prepared solution in a Teflon beaker was warmed to about 50 °C in a water bath, and then the cleaned glass was placed vertically into the solution for about 4 h. The deposited TiO_2 film was washed four times by using deionized water and dried at room temperature. The MIF was obtained after the imprinted template molecules were removed by one of three approaches. When no template was used, the obtained TiO_2 film was referred to as a non-imprinted film (NIF) as a control.

The three approaches of removing the imprinted template molecules were extraction, photocatalytic oxidation and calcination. In the extraction approach for removing the template molecules, the obtained films were washed five times by using 0.1 g L^{-1} Na_2CO_3 solution and distilled water in turn, which resulted in the removal of the template molecules from the film. In the photocatalytic oxidation for removing the template, the film was immersed in 10 mL water at pH 3 and irradiated under a 254 nm light source. Because of the intrinsic photocatalytic activity of the film, the template molecules were photodecomposed and finally removed. As the third approach, the film was calcined at 300 °C for about 2 h, and the calcination could decompose the template molecules and remove them. After the template molecules were removed with any of the three approaches, the MIFs were obtained as a selective photocatalyst.

2.3 Characterization

The profile of TiO_2 films was observed with a field-emission scanning electron microscope (FE-SEM, model S-4500, Hitachi). FT-IR and UV-visible solid-state reflection spectra were recorded on a Bruker VERTEX 70 spectrophotometer and a Shimadzu UV-2550 spectrophotometer, respectively. The surface diffractogram of the MIF was characterized by X-ray diffraction (XRD) on an X'Pert PRO X-ray diffractometer (PANalytical) with a Cu K_α radiation source.

2.4 Apparatus and methods

Adsorption experiments were conducted at 25 °C by immersing MIF and NIF films in a saturated SA solution (pH ≈ 2.7). After being immersed for 24 h, the films were taken out, cleaned by dipping in water, dried at 60 °C, and then analyzed by FT-IR to determine the relative adsorption amount of SA.

The photocatalytic experiments were performed in a 50 mL ringent photoreactor with a diameter of 9 cm. After two TiO_2 films were horizontally placed onto the bottom of the reactor, 25 mL solution of the specified organic compound(s) at pH 3.0 were added. A circlular 20 W UV light with an emission peak at 254 nm was horizontally positioned above the surface of the solution at a distance of 19 cm. After immersion for 20 min to achieve the adsorption–desorption equilibrium, the concentration of the pollutant(s) was determined as the initial concentration c_0, and then the photo-irradiation was started. At different time intervals, 2 mL aliquots were sampled to detect the pollutant and its degradation intermediates. When only SA was used as the pollutant to be degraded, UV-visible spectra of the supernatant with a quartz cell on a Shimadzu UV2501 spectrometer, and the SA concentration were obtained by using the absorbance at the maximum absorption wavelength of 296 nm according to the Beer–Lambert law. When SA and phenol were used as the mixed pollutants to be degraded, the concentrations of each pollutant in the mixture was analyzed by high-performance liquid chromatography on a PU-2089 HPLC (JASCO), equipped with a C18 ODS column and an ultraviolet detector. The mobile phase used was methanol–water (40 : 60 v/v) with a flow rate of 0.8 mL min^{-1}. The detection wavelengths were set at 296 nm for SA and 275 nm for phenol.

3. Results and discussion

3.1 Characteristics of photocatalysts

After the MIF and NIF films were scraped off the glass substrate, their diffuse reflectance UV-vis spectra were measured (Fig. 1). It is clearly seen from the spectra that the deposits in both the MIF and NIF have the UV-vis absorption characteristics of conventional nano-TiO_2 materials. The strong absorption in the UV region suggests that both MIF and NIF may be photocatalytic active under UV irradiation.

Fig. 2 shows FT-IR spectra of P25, SiO_2 and the MIF. The broad absorption peak of the MIF near 3454 cm^{-1} and a sharp peak about 1635 cm^{-1} are assigned to the stretching vibration of O–H hydroxyl groups and the bending vibration of coordinated Ti–OH or Si–OH, respectively.[19] Compared with the naked SiO_2, the peak at 1378 cm^{-1} is red shifted to

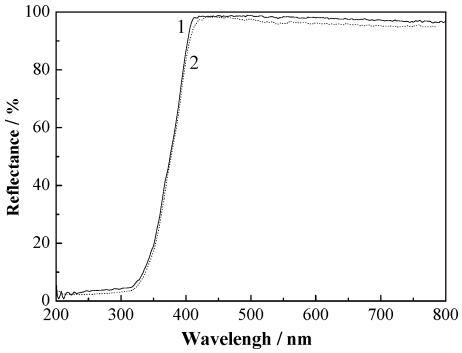

Fig. 1 Diffuse reflectance UV-vis spectra of MIF (1) and NIF (2).

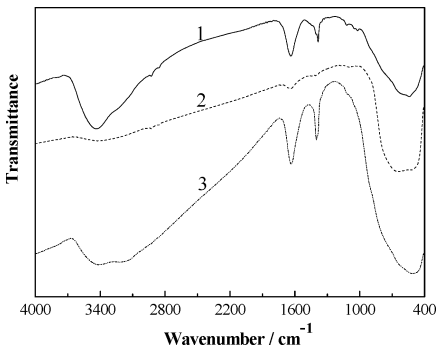

Fig. 2 FT-IR spectra of the MIF (1), neat P25 (2) and naked SiO_2 (3).

1399 cm^{-1} in MIF, being associated with the hydrogen bond between the Ti–OH hydroxyl group and the Si–OH hydroxyl group. This indicates that the coherence of the film to the glass substrate should be excellent due to the chemical bonding.

After the films were deposited in the presence and absence of P25 nanoparticles and calcined at 300 °C, their XRD patterns were recorded (Fig. 3). When the film was prepared in the absence of P25, the XRD pattern (curve 2) showed broad peaks at 2θ values of 25.5, 37.9, 48.2, and 54.5°, corresponding to the anatase TiO_2 structure. However, when P25 was added as seed during the preparation, the XRD pattern of the MIF was observed to have new peaks at 2θ values of 27.4, 54.0 and 68.9°, and these new peaks correspond to the rutile TiO_2 structure. P25 nanoparticles are a mixture of 80% anatase and 20% rutile, but the load of P25 nanoparticles in the deposition solution as the seeds was very small, and hence the amount of directly codeposited P25 nanoparticles in the MIF film was very little. Therefore, the markedly observed rutile structure is not from the codeposited P25 nanoparticle seeds, but from the effect of the seeds on the deposition of TiO_2 particles. The crystallization revulsant contributes to the formation of a mixed phase of anatase and rutile, which will enhance the photocatalytic activity of TiO_2.[20]

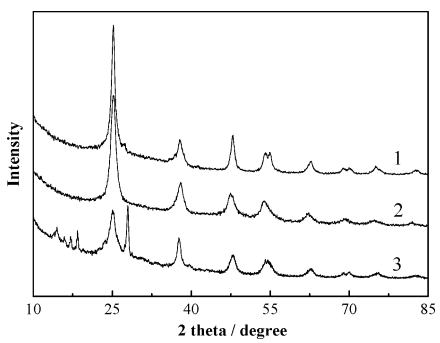

Fig. 3 XRD patterns of the imprinted TiO_2 films. (1) The film was prepared in the presence of P25 and then calcined at 300 °C, (2) in the absence of P25 and then calcined at 300 °C, (3) in the presence of P25 without any after-treatment.

Fig. 4 shows the surface morphology of MIF films obtained by three different methods of removing the template molecules. It is clearly seen that the MIF films prepared with the extraction and photodegradation methods have compact uniform surface, whereas the MIF obtained by removing the template with the calcination method has a porous morphology with a high surface area.

3.2 Effects of the methods of removing the template on the photocatalytic ability of the MIF

Three approaches were used to remove the imprinted template molecules from the deposited TiO_2 film. The first way is to extract SA by using Na_2CO_3 solutions as per the traditional method.[21–23] The second way was to remove SA by calcining the film at 300 °C. The heating temperature cannot be higher,

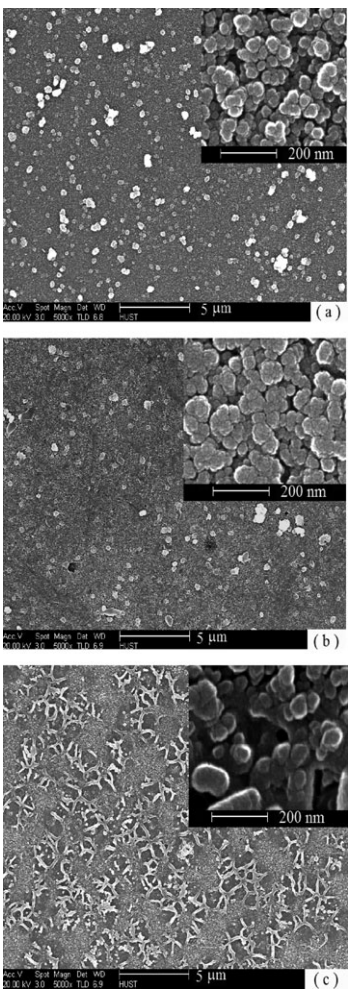

Fig. 4 The SEM microimages of the MIFs with the template removed by extraction (a), photodegradation (b) and calcination (c).

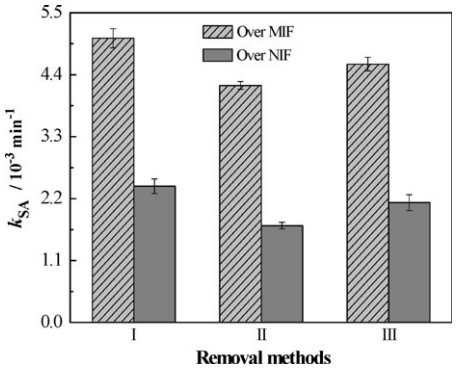

Fig. 5 Rate constants for the degradation of SA (25 mg L^{-1}) over MIF and NIF during a 180 min illumination. The removal of the template was achieved by calcination (I), photodecomposition (II) and extraction (III).

because a higher temperature will reduce the photocatalytic activity of the catalyst.[16,24] As the third way, the film was immersed in 10 mL water and UV irradiated under a 254 nm light source for about 12 h, which could mineralize the organic compounds by photocatalytic oxidation.

In our preliminary experiments, the photocatalytic decomposition of the organic pollutants used in the present work was found to follow a pseudo-first-order reaction in kinetics. Thus, the apparent rate constant k of the photoreaction was used to characterize the photocatalytic activity of the TiO_2 films and to evaluate the effects of specified conditions on the photocatalytic activity of the TiO_2 films. Fig. 5 shows the k values for the photocatalytic degradation of SA over the MIF films prepared by using different pretreatment approaches of removing the imprinted template molecules. Corresponding to the approaches of calcination, photodegradation and extraction, the k values over the MIF films are 0.00505, 0.00421 and 0.00438 min^{-1}, respectively. When the NIF films are similarly pretreated, the k values over the NIFs are 0.00242 min^{-1} (by calcination), 0.00172 min^{-1} (by photodegradation), and 0.00213 min^{-1} (by extraction). The selectivity of the MIF films, being defined as the ratio of the k value for SA over MIF to that over NIF, is 2.09, 2.45 and 2.06 for the template-removing approaches of calcination, photodegradation and extraction, respectively. Taking into consideration both the high degradation ability (k value) and selectivity, the calcination pretreatment was used for further experiments in the present work.

The methods of removing the template can influence the crystalline structure and surface morphology of the MIF. When the template is removed without calcination, some characteristic peaks of $(NH_4)_2TiF_6$ or its hydrolysis products (ammonium oxo-uorotitanates) are found, as shown in Fig. 3 (curve 3). This is indicative of incomplete crystallization under the experimental conditions.[25] However, after the MIF is calcined at 300 °C, these peaks disappear and the peak intensity for anatase TiO_2 is increased. Thus, the enhanced photocatalytic activity of the MIF is attributed to the increased amount of anatase TiO_2. Moreover, the morphology characterization in Fig. 4 demonstrates that the MIF obtained with the calcination method has a porous morphology with a high surface area. Therefore, more 3D "molecular footprint" cavities of the template are formed on the MIF prepared by calcination. This results in the higher photocatalytic activity of the MIF. Therefore, calcination at 300 °C is the best way among the three ways of removing the template for the preparation of efficient photocatalytic film photocatalyst.

3.3 Enhanced photocatalytic activity and selectivity of MIF

Fig. 6 gives kinetic data of direct photolysis and photocatalytic degradation of SA (10 mg L^{-1}) over the NIF and MIF, which show that all the degradation processes follow pseudo-first-order reaction kinetics. It is seen that the apparent rate for the direct photolysis of SA is slow, which indicates that the photolysis of SA is not efficient, agreeing with the recent report by Faramarzpour *et al.*[26] Because of the existence of TiO_2 and its photocatalytic ability, the photocatalytic degradation of SA over the NIF is fairly enhanced in comparison with the direct photolysis of SA. The molecular imprinting further promotes the photocatalytic activity of the deposited TiO_2 film. Accordingly, the apparent rate constant k of SA degradation over MIF (0.00959 min^{-1}) is about 2.5 times of that over NIF (0.00392 min^{-1}).

It is known that the adsorption of organic pollutants on the surface of a TiO_2 catalyst is one of the most important factors influencing their photocatalytic degradation.[27] Thus, the relative adsorption of the target pollutant on MIF and NIF was evaluated by using FT-IR (Fig. 7). In comparison with the neat TiO_2 film, the peaks at 1660, 1612 and 1467 cm^{-1} for both the MIF and NIF correspond to the C═O stretching vibration, benzene ring vibration and the stretching vibration of hydroxyl group of SA, respectively. The novel bands around 1294, 1242, 1210, 1154 and 1027 cm^{-1} are assigned to C–OH vibrations.[28] The changes observed in the IR spectrum of neat TiO_2 suggest that SA is bound to TiO_2 on both the MIF and NIF. Moreover, the absorbance of these peaks of SA in the spectrum of MIF are much higher than that of NIF, which means that the adsorption amount of SA on MIF is much more than that on NIF. The adsorption of SA is generally influenced by the solution pH because the solution pH affects the surface charge state of TiO_2 and the acid–base dissociation of SA. In the solution at pH 3.0 in the present work, the surface of TiO_2 films is positively charged since the pH is

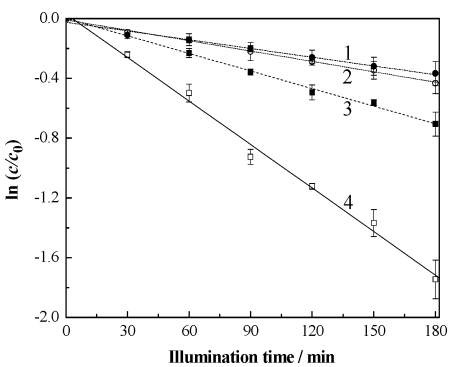

Fig. 6 Kinetics of direct photolysis (1) and photocatalytic degradation of SA (c_0 10 mg L^{-1}, pH 3) over the naked glass (2), NIF (3) and MIF (4).

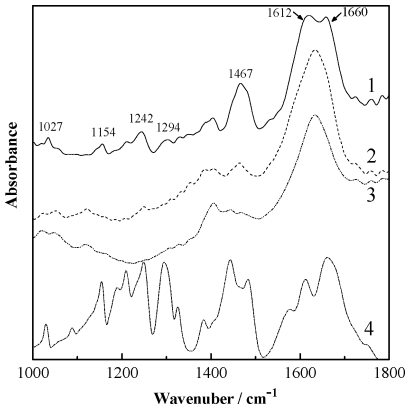

Fig. 7 FT-IR spectra of SA-adsorbed films of MIF (1) and NIF (2) in comparison with that of a neat TiO_2 film (3) and SA (4) as controls.

below the isoelectric point (at about pH 6.5).[29] This surface charge state favours the adsorption of negatively charged salicylicate ions. More salicylicate ions will be generated from the dissociation of SA at higher pH values. The contradictory requirements for the solution pH indicate that there is a favourable solution pH value. Therefore, the solution pH is selected at pH 3.0 in the present work because the pK_a value of SA is 2.97.[30] However, it is worthy noting that the enhanced adsorption on the MIFs is not from the appropriate solution pH, because the adsorption on the control NIF is carried out under the same conditions. Therefore, it is reasonable to conclude that the enhanced photodegradation of SA over MIF is attributed to its extraordinary recognition by the "footprint" of the catalyst, and the MIF is a promising photocatalytic film with the special adsorption ability for the target pollutant.

The photocatalytic degradation of SA is a complex process, which may be simplified as a combination of a series of steps, such as the adsorption of SA on the film catalyst, the photooxidation of the adsorbed SA, the desorption of the degradation byproducts, and the regeneration of the active surface of the photocatalyst. The total process can be analyzed with the Langmuir–Hinshelwood (L–H) model,[31,32] which is reported to be suitable for the photodegradation of a lot of organic pollutants on TiO_2.[33] In the present work, the SA solution was well stirred during the photodegradation, and the excellent mass transport conditions allowed us to have the following assumptions: (i) O_2 in the solution is always saturated; (ii) the photocatalytic activity of the film surface is alike; (iii) there is no difference between the interfacial concentration of contaminant and that in the bulk solution; (iv) the adsorbed SA molecules do not interfere with each other. With these assumptions, the reaction rate for the decomposition of SA on the surface of the photocatalyst can be expressed by eqn (1),

$$r = -\frac{dc}{dt} = k_r \frac{k_1 c}{1 + k_1 c} \quad (1)$$

where c is the SA concentration, k_r is the apparent reaction rate constant, and k_1 is the equilibrium adsorption constant of SA on the film. Because the used concentrations of SA are low (lower than 50 mg L^{-1}), it is reasonable to consider $k_1 c << 1$, and hence eqn (1) can be simplify to a pseudo-first-order reaction kinetic equation,[34]

$$r = -\frac{dc}{dt} \approx k_r k_1 c \quad (2)$$

This is well consistent with the pseudo-first-order kinetics observed experimentally in Fig. 6. According to Fig. 6, the photodegradation of SA over the immobilized TiO_2 films exhibits pseudo-first-order kinetics as follows:

$$r = -\frac{dc}{dt} = k_{obs} c \quad (3)$$

where k_{obs} is the apparent pseudo-first-order reaction rate constant. Thus, the relationship between k_{obs} and c can be expressed by eqn (4) and eqn (5).[35]

$$k_{obs} = k_r \frac{k_1}{1 + k_1 c} \quad (4)$$

$$\frac{1}{k_{obs}} = \frac{1}{k_r k_1} + \frac{c}{k_r} \quad (5)$$

The values of the adsorption equilibrium constant (k_1) and the apparent reaction rate constant (k_r) are obtainable by plotting the reciprocal of the apparent pseudo-first-order reaction rate constant ($1/k_{obs}$) as a function of the initial SA concentration (c_0), as shown in Fig. 8. For the MIF photocatalyst, these constants are obtained as k_1 = 0.968 L mg^{-1} and k_r = 0.125 mg L^{-1} min^{-1} (r^2 = 0.996), which are correspondingly much greater than that on NIF (k_1 = 0.133 L mg^{-1}, k_r = 0.083 mg L^{-1} min^{-1} (r^2 = 0.997)). That is, k_r and k_1 over MIF are 1.51 and 7.29 times that over NIF, respectively. This indicates that the target SA has a much higher affinity over MIF than that over NIF, which results in accelerated catalytic activity of MIF and is helpful to selectively remove low level SA from a mixed pollutants system.

The high selectivity of MIF towards the degradation of the target pollutant SA is confirmed by degrading the mixture of SA (2 or 25 mg L^{-1}) and phenol (25 mg L^{-1}). As shown in Table 1, when the concentration of SA is 25 mg L^{-1}, the rate constant of SA decomposed over MIF is 0.01189 min^{-1}, being twice that of the non-target phenol (0.00624 min^{-1}). When the degradation is carried out over NIF, the k value of SA is decreased to 0.00545 min^{-1}, being only 59% of that of phenol (0.00921 min^{-1}). The selectivity of MIF for SA is 3.24 in the

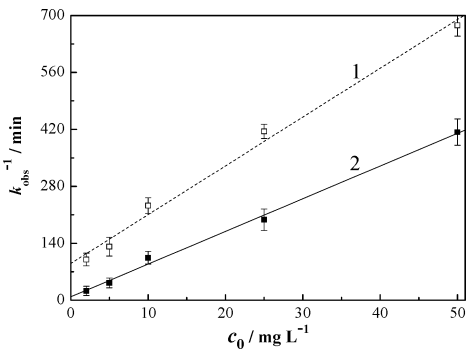

Fig. 8 Plot of the initial SA concentration (c_0) *versus* the reciprocal of the observed first-order rate constant ($1/k_{obs}$) over NIP (1) and MIP (2).

Table 1 Rate constants for the photodegradation of target SA (2 or 25 mg L^{-1}) in the presence of phenol (25 mg L^{-1}) over MIF and NIF[a]

	2 mg L^{-1} SA		25 mg L^{-1} SA	
	Over MIF	Over NIF	Over MIF	Over NIF
k_{target} (10^{-3} min^{-1})	23.88 ± 1.22	8.37 ± 0.24	11.89 ± 0.73	5.45 ± 0.55
$k_{non\text{-}target}$ (10^{-3} min^{-1})	7.04 ± 0.37	15.22 ± 0.65	6.24 ± 0.81	9.21 ± 0.48
R^b	3.39	0.55	1.91	0.59
α^b	6.16		3.24	

[a] Total illumination time was 180 min. [b] R is the ratio of $k_{target}/k_{non\text{-}target}$, and α is the ratio of the R value over MIF to that over NIF.

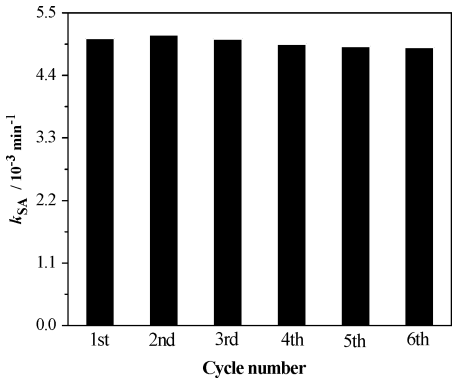

Fig. 9 Photocatalytic activity of the MIF in successive batches of SA photodegradation.

mixture of SA (25 mg L^{-1}) and phenol (25 mg L^{-1}). When the SA concentration is decreased to 2 mg L^{-1} in the mixture of SA (2 mg L^{-1}) and phenol (25 mg L^{-1}), the molecular recognition ability of MIF is better observed, and the selectivity of MIF is increased to 6.16. Thus, the selectivity of MIF towards the degradation of the target is increased with the decrease of the concentration of the target pollutant.

3.5 Stability of MIF during photocatalysis

The recovery and reuse of the photocatalyst are important in the photodegradation of organic pollutants. To evaluate the life time of MIF, the photodegradation of SA (25 mg L^{-1}) was carried out in successive batches. During this experiment, the MIF was simply recovered by taking it out of the solution because it was coated on the glass. In the first cycle, the degradation was conducted by irradiating for 180 min. After the film was rinsed with distilled water to remove the residual SA and byproducts, the pollutant solution was refreshed, and then the irradiation was continued again for 180 min as the second cycle of photodegradation. This process was repeated for several cycles. The k values for the first six cycles of photodegradation were determined in turn as 0.00505, 0.00511, 0.00504, 0.00495, 0.00491 and 0.00489 min^{-1} (Fig. 9). This indicates that the MIFs have excellent photochemical stability during the photodegradation process.

4. Conclusions

Using the improved LPD method with P25 as crystallization revulsant, we developed a novel approach for the preparation of photocatalytic thin films with high selectivity. Characterization with diffuse reflectance UV-vis, FT-IR, SEM and XRD indicated that the ways of removing the template molecules in the preparation of the MIFs mildly influenced the surface structure of the films. The calcination after-treatment was taken as the best way tested in the present work to remove the template molecules in the preparation of the MIFs. Because the molecular imprinting enabled the MIFs to have molecular recognition ability, the MIFs could selectively adsorb the target pollutant SA and promote the selective photocatalytic degradation of SA from its mixture solution with other organic pollutants. In the mixture solution, the selectivity of MIF toward the degradation of the target is increased with the decrease of the concentration of the target pollutant. Because of the high selectivity and excellent photochemical stability, the MIFs are promising in their applications for removing low-level target organic pollutants from complicated contaminated waters containing other pollutants.

Acknowledgements

The National Natural Science Foundation of China (grants no. 20677019 and 20877031) and the State Key Laboratory of Pollution Control and Resource Reuse Foundation (grant no. PCRRF08007) are greatly appreciated for the financial support of the work.

References

1 H. A. Seibel II, P. Karen, T. R. Wagner and P. M. Woodward, *J. Mater. Chem.*, 2009, **19**, 471.
2 T. Tachikawa, M. Fujitsuka and T. Majima, *J. Phys. Chem. C*, 2007, **111**, 5259.
3 S. Sato, R. Asahi, T. Morikawa, T. Ohwaki, K. Aoki and Y. Taga, *Science*, 2002, **295**, 626.
4 C. Feng, Y. Wang, Z. Jin, J. Zhang, S. Zhang, Z. Wu and Z. Zhang, *New J. Chem.*, 2008, **32**, 1038.
5 I. Sopyan, M. Watanabe, S. Murasawa, K. Hashimoto and A. Fujishima, *J. Photochem. Photobiol., A*, 1996, **98**, 79.
6 S. Li, R. Zhu, H. Zhu, M. Xue, X. Sun, S. Yao and S. Wang, *Food Chem. Toxicol.*, 2008, **46**, 3626.
7 J. A. Lee, K. C. Krogman, M. n. Ma, R. M. Hill, P. T. Hammond and G. C. Rutledge, *Adv. Mater.*, 2008, **20**, 1.
8 O. V. Makarova, T. Rajh and M. C. Thurnaure, *Environ. Sci. Technol.*, 2000, **34**, 4797.
9 V. Augugliaro, T. Caronna, V. Loddo, G. Marcí, G. Palmisano, L. Palmisano and S. Yurdakal, *Chem.–Eur. J.*, 2008, **14**, 4640.
10 K. Inumaru, T. Kasahara and M. Yasui, *Chem. Commun.*, 2005, 2131.
11 S. Ghosh-Mukerji, H. Haick, M. Schvartzman and Y. Paz, *J. Am. Chem. Soc.*, 2001, **123**, 10776.
12 S. Ghosh-Mukerji, H. Haick and Y. Paz, *J. Photochem. Photobiol., A*, 2003, **160**, 77.
13 X. Shen, L. Zhu, J. Li and H. Tang, *Chem. Commun.*, 2007, 1163.
14 X. Shen, L. Zhu, G. Liu, H. Yu and H. Tang, *Environ. Sci. Technol.*, 2008, **42**, 1687.
15 S. C. Lee, H. Yu, J. Yu and C. H. Ao, *J. Cryst. Growth*, 2006, **295**, 60.

16 W. Zhao, L. Zhou, C. Liu and L. Hu, *Acta Chim. Sin.*, 2003, **61**, 699, in chinese.
17 X. Z. Li, H. Liu, L. F. Cheng and H. J. Tong, *Environ. Sci. Technol.*, 2003, **37**, 3989.
18 L. Feng, Y. Liu and J. Hu, *Langmuir*, 2004, **20**, 1786.
19 M. M. Mohamed, T. M. Salama and T. Yamaguchi, *Colloids Surf., A*, 2002, **207**, 25.
20 Z. Wang, D. Xia, G. Chen, T. Yang and Y. Chen, *Mater. Chem. Phys.*, 2008, **111**, 313.
21 R. M. Garcinuño, I. Chianella, A. Guerreiro, I. Mijangos, E. V. Piletska, M. J. Whitcombe and S. A. Piletsky, *Soft Matter*, 2009, **5**, 311.
22 A. Katz and M. E. Davis, *Nature*, 2000, **403**, 286.
23 S. Fireman-Shoresh, S. Marx and D. Avnir, *Adv. Mater.*, 2007, **19**, 2145.
24 H. Wei, Y. Tsai, J. Wu and H. Chen, *J. Chromatogr., B: Anal. Technol. Biomed. Life Sci.*, 2006, **836**, 57.
25 N. M. Laptash, I. G. Maslennikova and T. A. Kaidalova, *J. Fluorine Chem.*, 1999, **99**, 133.
26 M. Faramarzpour, M. Vossoughi and M. Borghei, *Chem. Eng. J.*, 2009, **146**, 79.
27 D. Zhao, C. Chen, Y. Wang, H. Ji, W. Ma, L. Zang and J. Zhao, *J. Phys. Chem. C*, 2008, **112**, 5993.
28 L. Yang, Y. Xu, Y. Su, J. Wu, K. Zhao, J. Chen and M. Wang, *Spectrochim. Acta, Part A*, 2005, **62**, 1209.
29 S. Vilhunen, M. Bosund, M. Kääriänen, D. Cameron and M. Sillanpää, *Sep. Purif. Technol.*, 2009, **66**, 130.
30 C. Li, Y. Hsieh, W. Chiu, C. Liu and C. Kao, *Sep. Purif. Technol.*, 2007, **58**, 148.
31 M. V. P. Sharma, V. Durgakumari and M. Subrahmanyam, *J. Hazard. Mater.*, 2008, **160**, 568.
32 Y. Zong and J. J. Watkins, *Chem. Mater.*, 2005, **17**, 560.
33 M. Faramarzpour, M. Vossoughi and M. Borghei, *Chem. Eng. J.*, 2009, **146**, 79.
34 L. Luo, A. T. Cooper and M. Fan, *J. Hazard. Mater.*, 2009, **161**, 175.
35 M. Harir, A. Gaspar, B. Kanawati, A. Fekete, M. Frommberger, D. Martens, A. Kettrup, M. El Azzouzi and Ph. Schmitt-Kopplin, *Appl. Catal., B*, 2008, **84**, 524.